Journal of Structural Geology 33 (2011) 1751–1763

Contents lists available at ScienceDirect

Journal of Structural Geology

journal homepage: www.elsevier.com/locate/jsg

Review article

Quantitative analysis of crystal/grain sizes and their distributions in 2D and 3D

Alfons Berger [a,*], Marco Herwegh [b], Jens-Oliver Schwarz [c], Benita Putlitz [d]

[a] Institute of Geography and Geology, University of Copenhagen, Øster Voldgade 10, DK-1350 Copenhagen, Denmark
[b] Institute of Geological Sciences, University of Bern, Baltzerstr. 3, CH-3012 Bern, Switzerland
[c] Institute of Geosciences, University of Mainz, Becherweg 21, D-55099 Mainz, Germany
[d] Institut de Minéralogie et Géochimie, University of Lausanne, Bâtiment Anthropole 4140, CH-1015 Lausanne, Switzerland

ARTICLE INFO

Article history:
Received 13 December 2010
Received in revised form
5 July 2011
Accepted 17 July 2011
Available online 23 July 2011

Keywords:
CSD
Crystal sizes
Grain sizes
Mylonites
Porphyroblasts
Computed tomography
Image analysis

ABSTRACT

We review methods to estimate the average crystal (grain) size and the crystal (grain) size distribution in solid rocks. Average grain sizes often provide the base for stress estimates or rheological calculations requiring the quantification of grain sizes in a rock's microstructure. The primary data for grain size data are either 1D (i.e. line intercept methods), 2D (area analysis) or 3D (e.g., computed tomography, serial sectioning). These data have been used for different data treatments over the years, whereas several studies assume a certain probability function (e.g., logarithm, square root) to calculate statistical parameters as the mean, median, mode or the skewness of a crystal size distribution. The finally calculated average grain sizes have to be compatible between the different grain size estimation approaches in order to be properly applied, for example, in paleo-piezometers or grain size sensitive flow laws. Such compatibility is tested for different data treatments using one- and two-dimensional measurements. We propose an empirical conversion matrix for different datasets. These conversion factors provide the option to make different datasets compatible with each other, although the primary calculations were obtained in different ways. In order to present an average grain size, we propose to use the area-weighted and volume-weighted mean in the case of unimodal grain size distributions, respectively, for 2D and 3D measurements. The shape of the crystal size distribution is important for studies of nucleation and growth of minerals. The shape of the crystal size distribution of garnet populations is compared between different 2D and 3D measurements, which are serial sectioning and computed tomography. The comparison of different direct measured 3D data; stereological data and direct presented 2D data show the problems of the quality of the smallest grain sizes and the overestimation of small grain sizes in stereological tools, depending on the type of CSD.

1. Introduction

In the past years, the importance of the description of crystal-, grain- or particle-sizes increased in terms of quantitative parameterization of microstructures (see Vernon, 2004; Higgins, 2006; Jerram and Kent, 2006; Jerram and Higgins, 2007; Herwegh et al., in this volume; Fig. 1a). Such information on crystal/grain sizes and their distributions are often combined with other quantitative microstructural parameters, as the distance to the nearest neighbours, crystal shapes, shape preferred orientations (SPO) or volume fractions of phases (e.g., Boorman et al., 2004; Brodhag et al., 2011; Herwegh et al., 2005, in this volume). The term "crystal size" is often used to describe the dimensions of minerals in the petrological community (e.g., Marsh, 1988; Higgins, 2006); whereas structural geologist and material scientists often use the term "grain size" (e.g., Schmid, 1975; Rutter, 1995; Kohlstedt et al., 1995). Note that both terms are synonyms and we therefore try to use the terms in accordance to the field of their applications. Crystal- or grain size refers to the size of a certain mineral or solid phase of comparable chemical composition. In contrast, the term particle is used for more complex solid aggregates and often the composition of the particle can vary (e.g., Storti et al., 2003).

In addition to the classical static growth of minerals driven by a reduction of surface energy, dynamic recrystallisation via grain boundary migration is an important grain size controlling mechanism inducing synkinematic grain growth during deformation (e.g., Hirth and Tullis, 1992; Gleason et al., 1993; Stipp et al., 2010; Platt and Behr, 2011 and reference therein). Alternatively grain sizes can also be synkinematically reduced via subgrain rotation

* Corresponding author. Tel.: +45 35322439; fax: +45 35322501.
E-mail addresses: ab@geo.ku.dk (A. Berger), herwegh@geo.unibe.ch (M. Herwegh), schwarj@uni-mainz.de (J.-O. Schwarz), Benita.Putlitz@unil.ch (B. Putlitz).

0191-8141/$ – see front matter © 2011 Published by Elsevier Ltd.
doi:10.1016/j.jsg.2011.07.002

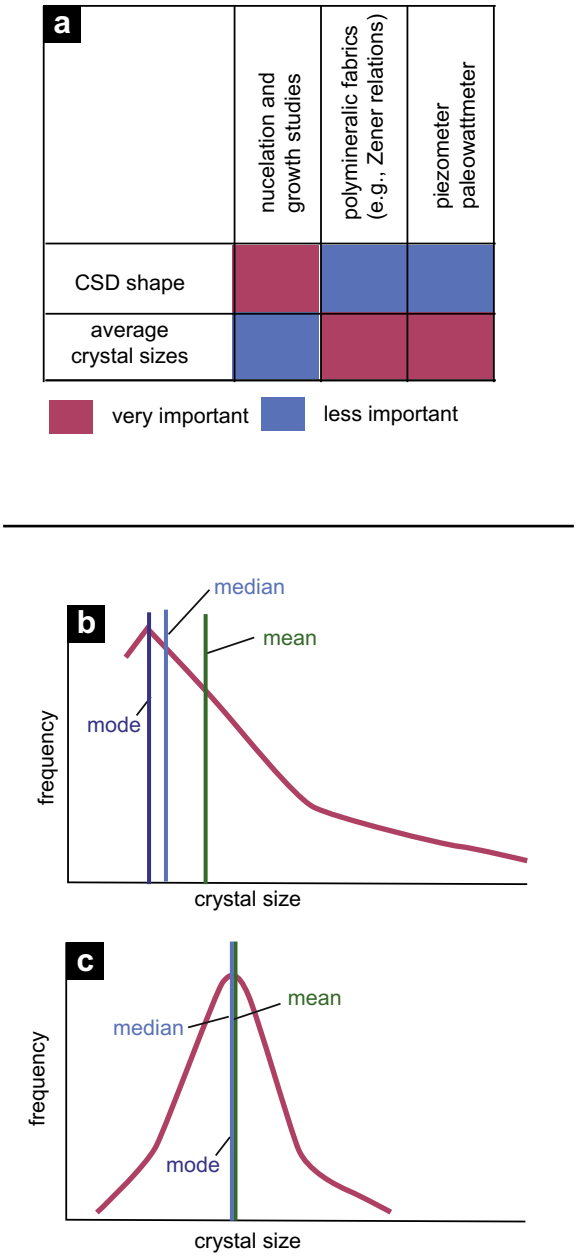

Fig. 1. (a) Applications and relevance of CSD and average crystal sizes in different research fields of earth and material science; (b) schematic CSD characterized by nucleation and grain growth and; (c) schematic bell-shaped CSD both showing the relation to the mean, mode and the median.

recrystallisation. In this case problems with respect to the proper definition and exact location of the grain boundary can arise, where misfits of 10–15° between adjacent crystallographic compartments are used to define high angle grain boundaries, i.e. independent grains (Poirier, 1985).

The quantification of microstructures includes the estimation of average crystal sizes as well as crystal size distributions (CSD). In general, the theoretical backgrounds for crystal size analysis are: (1) nucleation and growth of minerals in a melt; (2) stabilized grain sizes in ductile deformed materials and (3) grain coarsening processes in solid materials. The techniques and theoretical background of (1) have been also transferred to metamorphic rocks (e.g., Cashman and Ferry, 1988; Carlson, 1989, 2010, Berger and Roselle, 2001). These topics will be shortly introduced in the following.

1.1. Grain size during nucleation and growth

In the case of polymineralic metamorphic rocks, nucleation and growth processes of individual minerals on one hand side and grain coarsening processes of the entire aggregate on the other side often occur at the same time in both static and deformed metamorphic rocks (Berger et al., 2010; Brodhag et al., 2011; Herwegh et al., in this volume). Nucleation and growth processes have been analyzed successfully in volcanic rocks (e.g., Cashman and Marsh, 1988; Marsh, 1998; Higgins and Roberge, 2007). In this research field, the crystal size distribution is presented as the population density diagram (see Marsh, 1988 and Randolph and Larson, 1971 for theoretical background). This type of CSD presents the ln of the population density versus crystal size classes. The resulting CSD are examined in terms of the nucleation density, growth rate, but also parameters as the average crystal sizes can be extracted (e.g., Marsh, 1988; Higgins, 2006). This type of the CSD analysis is developed for single crystals embedded in an infinitely large matrix, as phenocrysts in a melt. To obtain a profound insights on nucleation and growth processes information on nucleation density and growth rate are required, which can be extracted from a CSD. In addition, the knowledge obtained from the volcanic rocks, i.e. from the melt-crystal system, was also adapted to metamorphic rocks (e.g., Cashman and Ferry, 1988; Carlson, 1989; Denison and Carlson, 1997; Denison et al., 1997).

1.2. Coupled grain growth

In addition to nucleation and growth, aggregates often are overprinted by different coarsening processes (e.g., De Hoff, 1991; Miyazaki, 1991; Miyake, 1998; Herwegh and Berger, 2003; Berger and Herwegh, 2004). The background for grain coarsening is given in Evans et al. (2001), which describe the change of the average crystal size in a complete solid system. However, in most natural examples of polymineralic rocks, the minerals underwent coupled grain growth (see Fig. 1 in Berger et al., 2010 for nomenclature). In addition, for investigations on polymineralic, metamorphic microstructures, the role of the matrix microstructure on the growth of new phases, like porphyroblasts, becomes more and more obvious (e.g, Carlson and Gordon, 2004; Berger et al., 2010). The study of the evolution of the matrix crystal sizes and crystal sizes of newly formed mineral reaction products requires the combination of CSD data and average crystal sizes (Berger et al., 2010; Herwegh et al., in this volume). For example, the interactions of different mechanisms of nucleation and growth versus coarsening can be unravelled on the base of CSDs, average crystal sizes and their statistical parameters (e.g, Eberl et al., 1998, 2002; Kile et al., 2000; Berger and Herwegh, 2004).

1.3. Grain sizes in deformed material

In the research field of rock deformation, the average grain size is a key variable in the context of grain size sensitive flow (e.g., Schmid et al., 1980; Walker et al., 1990; Platt and Behr, 2011), paleopiezometry (e.g., Twiss, 1977; Gleason and Tullis, 1993; Rutter, 1995; Herwegh and Handy, 1996; Shimizu, 1998; Post and Tullis, 1999; Stipp and Tullis, 2003; Stipp et al., 2010) or energy based considerations of deformation like the paleowattmeter (Austin and Evans, 2007, 2009). Experimental and natural data show that the mechanical and structural steady state evolve at a rate uniquely defined by the recrystallized grain size in deformed rocks, which is related to cyclical growth and grain size reduction of individual grains (Means, 1981, see review in Herwegh et al., in this volume). Different aspects are known for grain size reduction and grain growth mechanism in monomineralic systems (De Bresser et al.,

1998, 2001) and polyphase systems (Herwegh et al., in this volume). Different studies show the influence of the grain size on the behaviour of such mylonites (e.g., Hobbs, 1968; Herwegh et al., 2005). All these applications require the extraction of an average crystal size of a polycrystalline aggregate with specific CSD. In such deformation related studies, the CSD often are presented as histograms, where the frequencies of different grain size classes are displayed.

2. Description of measurement techniques

2.1. Overview of methods

In order to quantify crystal sizes and the crystal size distributions, a broad variety of different analysis techniques and approaches have been applied in the past decades. This is problematic, since such data have been used to calibrate experimentally derived data (e.g. flow laws, piezometers) allowing extrapolation to natural conditions. Principally such extrapolations are only valid, if the microstructures of the natural samples are analysed in the same manner as was the case for the experiments. Given the aforementioned progress in analysis techniques, however, this requirement sometimes failed for grain size data, where nowadays with reduced effort statistically much more reliable datasets can be generated.

Despite of different data treatment, which will be discussed below, the primary data can be separated into three groups: (1) 1D data (i.e. line intercept methods, number of grains per unit area); (2) 2D data (area estimation using different image analysis tools); (3) 3D methods (computed tomography, serial sectioning). 1D data mainly were used in previous times when manual counting was required for grain size estimations. Most simple is the counting of the number of grains per unit area, where the division of the unit area by the number of grains results in an average grain area. With the linear intercept method, the number of grain segments along a given line is detected, for which again the length of the line divided by the number of segments yields a grain size estimate. Note that in case of both approaches just single grain size values were obtained without any statistical information on grain size variations. A large variety of methods are proposed to detect individual 2D and 3D grains and related grain boundaries (e.g., hand drawing, EBSD, filtering of digital images). Independent of different data processing, the quality of the raw data is related to aforementioned methods. In general, most primary data are based on digital images, where the quality is mainly related to the chosen resolution (see details below). Independent of the selected method, the proper statistical treatment requires a certain number of grains. A detailed analysis of the robustness of CSD is given in Morgen and Jerram (2006). A number of at least 200–250 grains are necessary to obtain robust information on a CSD and the average grain size (see also below). However, a larger number of individual grains is of advantage.

2.2. Specific methods

This contribution discusses the role of the quality of grain size estimates in general, but concentrates on a metapelitic sample using the crystal size measurements of garnets (Schwarz, 2008; Schwarz et al., 2011) and carbonate minerals in mylonites (Fig. 2; Herwegh et al., 2005, 2008; Ebert et al., 2007, 2008). The used metapelite sample is a porphyroblastic schist, comprising garnet, staurolite, kyanite, plagioclase, muscovite, paragonite, biotite and quartz. Garnet forms euhedral to subhedral porphyroblasts. The petrology of the sample is described in detail in Schwarz (2008). We also present data from a sample series of carbonate mylonites from the Doldenhorn nappe, which are described in detail by Herwegh and Pfiffner (2005) and Herwegh et al. (2005). The estimation of the garnet crystal size includes three techniques: (1) analysis of 2D surfaces; (2) serial sectioning (3D), (3) x-ray computed tomography (3D). The 2D data of garnets and calcites were measured by image analysis.

The carbonates were in generally measured on rock chips or thin sections (e.g., Herwegh and Berger, 2003, 2004; Berger and Herwegh, 2004; Herwegh et al., 2008; Ebert et al., 2007, 2008). Several of these samples were prepared by the two-step etching approach (Herwegh,

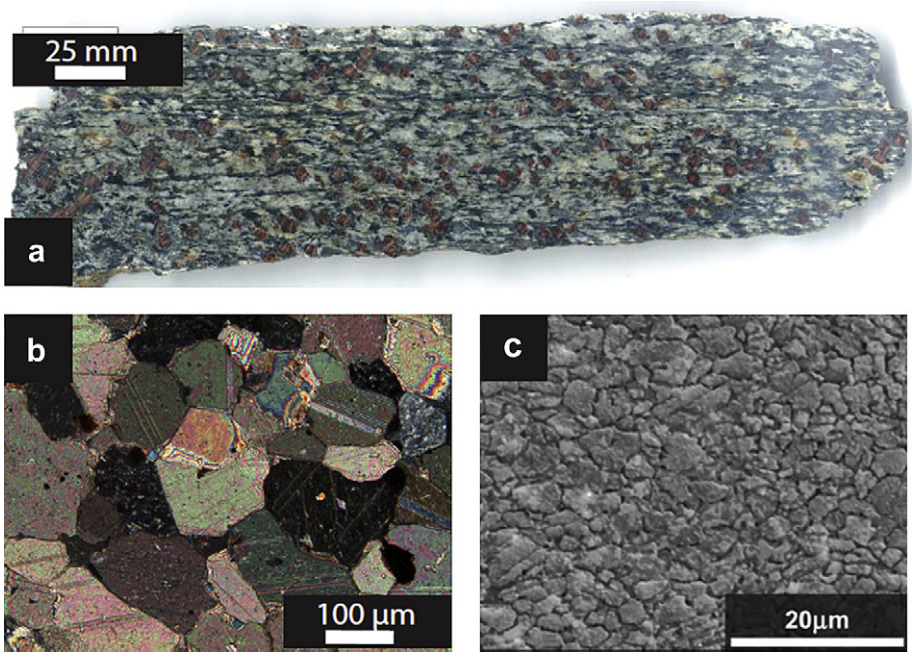

Fig. 2. Different samples and applied crystal size measurement techniques: (a) polished hand sample used for the drawing of garnet crystals and the estimation of their CSD; (b) thin section photograph of the microstructure of a metamorphic carbonate; (c) microstructure of a carbonate mylonite visualized by two-step etching and BSE imaging (see Herwegh, 2000).

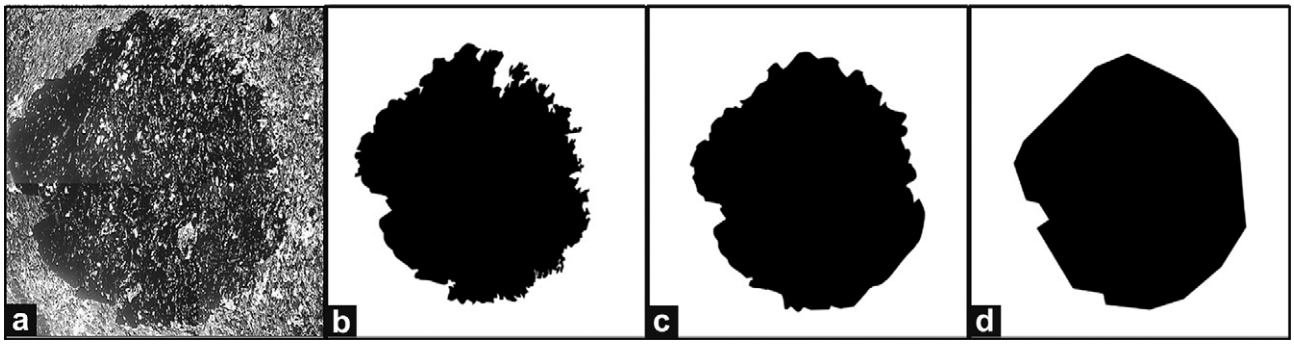

Fig. 3. Grain outlines of a garnet produced at different magnifications to illustrate the effect of scaling on the uncertainties of grain measurements (see also Table 1). (a) Image of the used garnet; (b) high resolution applied to reproduce the image of a single garnet crystal by a mosaic comprising of different images; (c) magnification used to resolve a single garnet crystal; (d) application of a low magnification to cover several garnet crystals at once.

2000). Digital images of the planar surfaces were captured in backscatter electron mode on a SEM. Based on these images, grain boundary outlines were generated and the areas, perimeters, short and long axes of the grains were calculated using *NIH Image* or *Image SXM* (see references in Herwegh, 2000). In light of grain size analysis it is important to note that (a) measurements were based on pixels and (b) the measured grain areas had to be corrected by adding the perimeter of a grain to the originally measured grain area. The latter treatment is necessary, because of a constant grain boundary width of 2 pixels, which is not included in the area measurement. Linear intercepts were quantified for horizontally and vertically oriented grid lines using a macro that allowed adjustment of the grid spacing at the beginning of each run.

For the garnet, grain boundary outlines were hand traced on polished rock slabs. The digitized garnet grains and the rock slab were analyzed for area and coordinates of garnet grains with *ImageJ* (Version 1.34s) as described before for the calcites. 2D grain sizes of garnet porphyroblasts (and thus 2D CSD) are generated using the same technique as described above. We apply two stereological correction methods to the 2D data: (a) an iterative approach based on the Schwartz-Saltykov method (Underwood, 1968). This 3D extrapolation procedure is available as a FORTRAN code called "*StripStar*", which is described in Heilbronner and Bruhn (1998). (b) Higgins (2000) provides a method, which also accounts for the shape of particles and the fabric of the rock. This correction method is available as the program "*CSDCorrections*".

For serial sectioning, we generated numerous parallel surfaces by multiple grinding and polishing of a rock slab (e.g., Bryon et al., 1995; Cooper and Hunter, 1995; Kretz, 2006; Mock and Jerram, 2005). The sizes of garnet crystals on each of the surfaces were quantified with *ImageJ* as described above. The rock slab is then ground down by 50 μm, parallel to the existing surface. Because the minimum garnet grain size is on the order of several 100 μm, every garnet crystal is encountered and sectioned multiple times. From the created 2D cuts of a garnet grain the "true" grain size in 3D was determined. The 3D grain size corresponds to the cut that passes through the garnet centre or that comes closest to it. Because of the large number of 2D cuts of garnets, a FORTRAN program was written to help in identifying the centroid cut of each grain and to compute its 3D grain size. The program corrects artefacts related to both touching of grains and edge effects. We also measured 3D garnet CSD directly by computed tomography. Geometrical properties of garnet porphyroblasts in 3D were analyzed using the Skyscan 1072 microtomograph at the University of Lausanne (Switzerland). Cylinders 1.6 cm in diameter and 3.7 cm in height were drilled out of the sample and used for measurements. Spatial resolution of the computed tomography measurements is determined by the voxel size, which is ~19 μm (edge length of the voxel cube, i.e. the pixel equivalent in volume). Results of the computed tomography analyses are given as a set of sectional contiguous greyscale images, which reproduce the variations of the X-ray attenuation within the sample. X-ray attenuation is closely related to the material density. Hence the generated sectional images visualize variations in density. These images are then compiled to create a 3D representation of the sample, using the program "*BLOB3D*" by Ketcham (2005).

Subsequently individual garnet grains have to be identified in the dataset and their geometrical properties have to be determined. This is done by the following steps. (1) Segmentation: all voxels of the dataset that belong to the phase of interest are identified and extracted by a user defined greyscale range for this phase. (2) Separation: after segmentation, the remaining voxels form groups of three-dimensional connected voxels (blobs) that represent individual grains and cluster of grains. Due to the idiomorphic character of the garnet prophyroblasts, the later are easy to identify and to separate in *Blob3D*. If all blobs are separated into individual grains, their geometrical properties (e.g. grain size, volume etc.) are computed. Despite the clear density contrast between garnet and other porphyroblastic phases in the sample, segmentation produced many artefacts that had to be removed by hand. The artefacts derive mainly from voxels that represent mineral mixtures with a mean

Table 1
Data of area and perimeter estimates depending on the quality of grain boundary detection (see Fig. 3).

	Area [mm^2]	Rel. diff to draw. (1) in %	Perim. [mm]	Rel. diff to draw. (1) in %
Drawing 1	11.35		25.82	
Drawing 2	11.61	2.29	15.81	38.76
Drawing 3	11.58	1.97	13.43	47.96

Table 2
Uncertainties of repeated measurements of garnet in sample SPi0306.

Grain	Average grain size [mm]	Error [%]	STDV
1	1.0251	1.48	0.0107
2	1.1992	1.70	0.0126
3	1.5288	1.20	0.0134
4	1.3935	0.65	0.0061
5	0.8205	3.98	0.0204
6	1.5680	0.67	0.0070
7	0.2503	14.84	0.0254
8	0.5971	3.73	0.0130
9	0.2289	8.83	0.0111
10	2.2623	1.77	0.0257

Table 3
The discussed ways to calculate average crystal size.

	Nr. weighted grain size distribution	ln grain size distribution	*SQRT* grain size distribution	Area weighted grain size distribution
Individual crystal size	$d_i = 2\cdot\sqrt{\frac{A_i}{\pi}}$	$d_{\ln(i)} = \ln\left(2\cdot\sqrt{\frac{A_i}{\pi}}\right)$	$d_{sqrt(i)} = \sqrt{2\cdot\sqrt{\frac{A_i}{\pi}}}$	$d_i = 2\cdot\sqrt{\frac{A_i}{\pi}}$
Frequency (ϕ_j) per grain size class $w = d_{\max}/j$	$\phi_j = \sum_{d_i>w_{j-1}}^{d_i<w_j} \frac{n_i}{n_{tot}}$	$\phi_j = \sum_{d_{\ln(i)}>\ln(w_{j-1})}^{d_{\ln(i)}<\ln(w_j)} \frac{n_i}{n_{tot}}$	$\phi_j = \sum_{d_{sqrt(i)}>\sqrt{w_{j-1}}}^{d_{sqrt(i)}<\sqrt{w_j}} \frac{n_i}{n_{tot}}$	$\phi_j = \sum_{d_i>w_{j-1}}^{d_i<w_j} \frac{A_i}{A_{tot}}$
Mean grain size ($\bar{d}$)	$\bar{d} = \sum_{i=1}^{n_{tot}} d_i \Big/ n_{tot}$	$\bar{d} = \exp\left(\sum_{i=1}^{n_{tot}} d_{\ln(i)} \Big/ n_{tot}\right)$	$\bar{d} = \left(\sum_{i=1}^{n_{tot}} d_{sqrt(i)} \Big/ n_{tot}\right)^2$	$\bar{d} = \frac{w}{\sum_{i=1}^{n_{tot}} A_i} \cdot \sum_{j=1}^{j_{tot}} \left(j\cdot \sum_{i=1}^{i} A_{ji}\right)$

With A_i: area of the ith grain; A_{tot}: the total grain area of the aggregate ($A_{tot} = \sum_{i=1}^{n_{tot}} A_i$) d: *equivalent circular diameter*; n_{tot}: total number of measurements; n_i: number of measurements per grain size class; j_{tot}: total number of grain size classes; w: class width.

density close to garnet. Artefacts and garnets are distinguished based on shape (garnet forms idiomorphic porphyroblasts) and grain size (artefacts are order of magnitude smaller than the smallest garnet grain identified by optical microscopy). After separation, the geometrical properties (volume and coordinates of object center) of the defined objects were measured by the program *BLOB3D*.

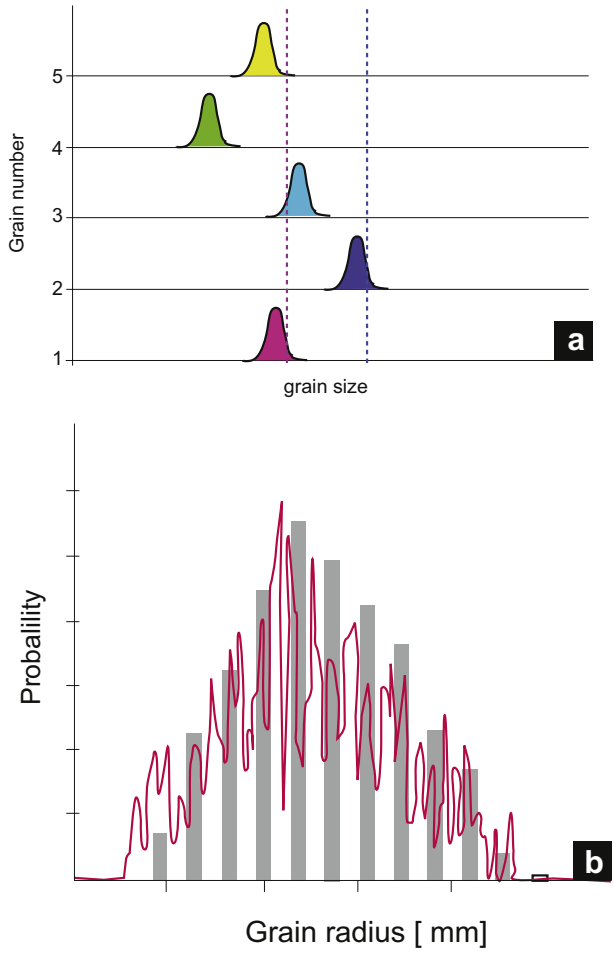

Fig. 4. (a) Schematic illustration for the calculation of the total probability value. The total probability value for a specific grain size is computed by summation of all function values present at a specific grain size (purple dashed line). In the depicted case grains 1, 3 and 5 would contribute to the total probability function at the grain size marked by the dashed line. For another grain size (blue dashed line), only grain number two contributes to the total probability value. (b) Thin line represents the garnet CSD with representation of errors on the individual grain size measurements (see (a)). The values of the bin-size from Fig. 7a are shown for comparison.

3. Discussion

3.1. Uncertainty of measurements and transferring it to a CSD

Independent of the used method, every individual grain size measurement has an error. The most common methods are restricted to the 2D space and are based on image analysis (e.g., Herwegh, 2000; Heilbronner, 2000; Bjørk et al., 2009; Brodhag et al., 2011). The base to estimate the areas in 2D sections are often (1) EBSD data; or (2) line drawings from thin section or rock slabs. In addition, also automated image analysis has been proposed (e.g., Barraud, 2006; Bjørk et al., 2009). The uncertainty of the estimated area using image analysis depends strongly on the selected magnification and related image resolution. Detecting irregular grain boundaries in 2D or 3D would require local high resolution imaging, which cannot generally be applied during measurements of a large number of crystals, because of scaling problems. In order to estimate the role of grain boundary resolution, we use one garnet prophyroblast and measure the area in drawings performed at different resolution. Note that for this approach we applied high magnification to focus on the grain boundary only (Fig. 3a) as well as low magnifications at which several garnets grains can be drawn (Fig. 3c). The resulting loss in resolution of the grain boundary structure is shown by the change of the grain perimeter (Fig. 3; Table 1), which is substantial the lower the magnification becomes. At the same time, however, the error on the calculated grain area (grain sizes) is low (Fig. 3; Table 1). This scaling problem will occur for different techniques and results in severe problems when considering grain surfaces.

Looking at grain size evolutions using mean grain sizes in the case of large-scale temperature gradients, often considerable grain size variations ranging from the micrometre up to the centimetre scale have to be covered by the measurement. No unique analysis technique can be used for grain size estimations of the entire range, requiring the application of different methods, each suitable for a proper analysis in terms of both the resolution of an individual grain and a statistically satisfying number of grains at the given magnification. For this purpose analysis techniques on the micrometre scale (Scanning electron microscopy), tens of micrometre to millimetre scale (optical light microscopy) and centimetre scale (low magnification digital imaging) need to be combined with each other (e.g. Berger and Herwegh, 2004; Ebert et al., 2010). This is a challenging task since the errors ranges should stay in a similar range compared to the individual mean grain size for all the methods.

Digitization of the rock slab or thin section may result in different sources of analytical errors. These are mainly related to the precision of hand tracing of the boundary between grains and matrix. In addition, during the transfer into a bitmap, the definition of the pixels include uncertainty. The individual errors are correlated and errors are best estimated by experimental data. In order

to estimate the magnitude of these errors, we selected a metapelite sample and measured several hundreds of garnets on a polished rock slab. We evaluated the errors from repeated measurements on several grains, because potential variations are the result of the hand-tracing process and the following digitization procedure. Repeated measurements indicate that the relative error depends again on the resolution. This procedure is important, because the application of average crystal size or CSD data is only possible by incorporating the whole grain population into the analysis. The spreads between individual grains could be in the range of a factor of ten, because of 2D sectioning effects and natural variations in grain size. Therefore, it is nearly impossible to adapt the resolution for individual grains inside an aggregate (using rock slabs, thin sections or rock piece in CT). Therefore, optimizing resolution for the mean grain sizes results in considerable errors for the smallest grain sizes (Morgan and Jerram, 2006). The repeated measurements in our example indicate an error in grain size between 1 and 4% and a maximum error for the small grains of 15% (Table 2; see Gualda, 2006).

For data presentation, errors related to individual grain sizes have to be transferred to population density or frequency diagrams. In all these presentations and statistical treatments, each grain size measurement must be assigned to a specific grain size class. This disregards the uncertainty in data and introduces ambiguity because the errors of measurement, as shown above, are non-negligible and may exceed commonly used bin widths. The choice of bins thus impairs the assessment of the uncertainty in the distribution, as histograms do not reflect the measurement error, which itself is grain size dependent. An improved representation of the CSD is achieved by converting the primary data into a probability distribution, as follows: Each grain size measurement is represented by its estimated uncertainty, which is assumed to be distributed normally around the measured value. These individual Gaussian shape uncertainties are then summed over all of the grains of one sample to obtain its CSD. In other words, the total probability value for a specific grain size is computed by summation of all function values present at a specific grain size (see red line in Fig. 4). Such a generated CSD that accounts for individual errors on grain size measurements is displayed in Fig. 4b. The resulting probability curve is controlled by changing numbers of grains with a similar grain size and are not artifacts related to the allocation of grains to certain grain size intervals. The resulting wiggly appearance of the CSD is related to the width of normal distributions representing a grain size measurement and the associated error. Apparently, estimated errors are not big enough to create larger overlaps between individual normal distributions and so produce the wiggly appearance of the graph. Such consideration on the CSD error is important in the case of bimodal CSD (Fig. 5). Bimodal distributions can be expected in deformed rocks (see section below) and during heat-flow controlled garnet growth (Schwarz et al., 2011). In addition, also the combination of coarsening and nucleation and growth may lead to bimodal distributions. The identification of bimodal CSDs can be difficult and depends on the error and the number of the grain size classes. A discussion on size class error is therefore necessary to extract robust information from bimodal CSDs (Fig. 5).

3.2. Comparing 2D and 3D measurements

In order to test different grain size analysis techniques in 2D and 3D and available stereological methods, we use a sample with garnet porphyroblasts (see description above) to compare the following methods: (1) 2D data based on image analysis, (2) 3D data based on data from serial sectioning, (3) 3D data measured by

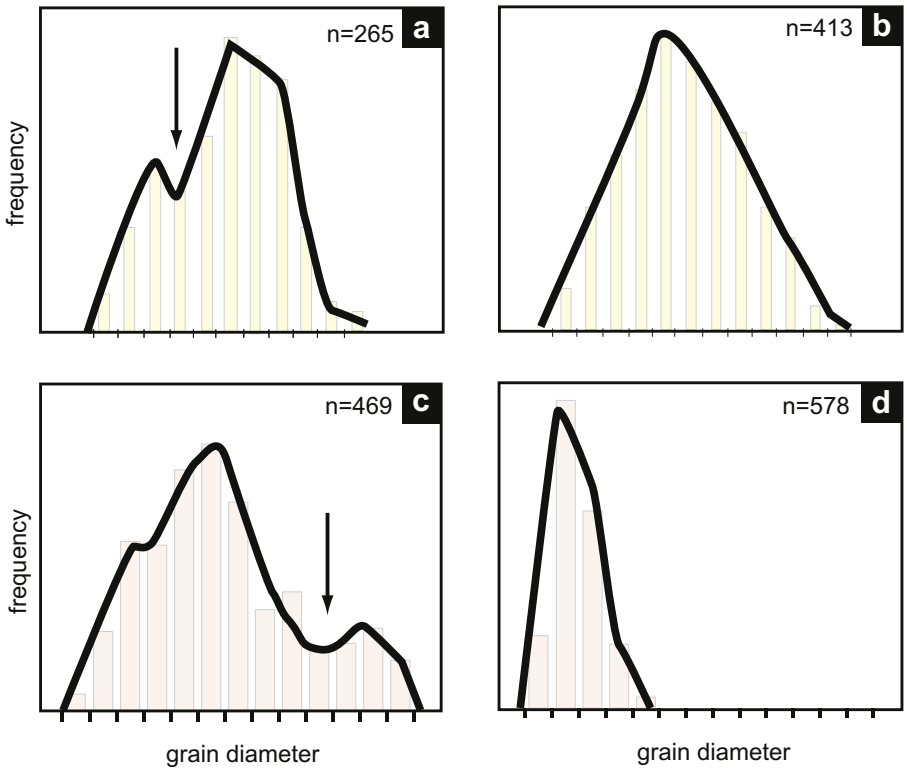

Fig. 5. Examples for detailed examination of the CSD. (a and b) garnet CSD (Schwarz, 2008); (c and d) calcite mylonites (redrawn after Ebert et al., 2007). (a) CSD of sample SDe0303, note the bimodal distribution. (b) Unimodal CSD of sample SPi0306, compare Fig. 7. (c) CSD from mylonites with bimodal distribution and large width of CSD. (d) CSD from mylonites with unimodal distribution and small width of CSD.

computed tomography and (4) stereological calculations on the base of the measured 2D data. Results for the generation of a CSD of the metapelite sample from the different techniques are compiled in Figs. 6 and 7 and Table 4. The different techniques mentioned before show clear differences in the resulting CSD. The CSD based on the uncorrected 2D data displays a typical bell-shaped CSD of garnet (Fig. 6a). The CSD generated based on 3D data from stereological conversion programs show remarkable differences compared to the other approaches. Both conversion programs (*CSDcorrections*: Fig. 6b; *Stripstar*: Fig. 7b) yield a distinct increase in the grain size fraction present in the smallest bins. In Fig. 7b this increase is indicated by the occurrence of negative values for the frequency, which denotes a lack of grains in these bins to enable a correct conversion of 2D to 3D data. The same increase is directly visible in the CSD computed by "*CSDcorrections*" (Fig. 6b). In contrast to these restrictions of the 3D conversion programs, the CSD generated based on true 3D data does not show this increase in the smallest grain size classes. Further comparison of the CSD exhibit differences in the minimum and maximum grain size that are attributed to the different numbers of grains involved in the generation of the CSD and to the intersection-probability effect (Higgins, 2000) for the 2D CSD. In total the accordance between CSD based on 2D and 3D data is better than between CSD from 3D data and converted 3D data. Moreover, CSD computed on the basis of 2D data reproduces crucial characteristics (e.g. shape of the CSD, average grain size) of the CSD based on 3D data quite well (Table 4) in comparison with stereological reconstructions.

3.3. Correlate different methods

Average grain sizes have been used for different investigation, as for example, grain size evolution with coarsening or paleopiezometry (see Herwegh et al., in this volume and references therein). Owing to limitations of manual analytical techniques, in many older studies, crystal sizes are given as a 1D length. A 1D value therefore either describes the average intersection length of an arbitrarily passing through the grain aggregate or the grain size determined by the mesh size of a sieve. In crystalline rocks also sieves were used to estimate the crystal sizes (Jones and Galwey, 1966; Galwey and Jones, 1963). Later, intercept methods became more common to estimate the grain size (e.g. Exner, 1972; Srivinansan et al., 1991). However, modern methods are often based on image analysis (see Higgins, 2006 and literature therein), and estimate the sectional area (2D) or the volume of a grain (3D). These primary 2D or 3D area or volume data are converted back into an individual 1D length (Table 3). This reduction is often done via the equivalent circular or spherical diameter by:

$$\text{in 2D}: d = 2^{*}\sqrt{\frac{\text{area}}{\pi}} \quad (1)$$

$$\text{or 3D}: d = 2^{*}\sqrt[3]{\frac{3}{4}{*}\frac{\text{volume}}{\pi}} \quad (2)$$

with d: diameter (or the radius ($r = d/2$) is used).

This conversion assumes a circular (2D) or spherical (3D) shape of the crystals. The transformations are becoming more problematic for minerals with more complex geometrical shapes in 2D or 3D (e.g. Higgins, 2000; Gualda, 2006; Morgan and Jerram, 2006). For example, the stereological extrapolations between 2D and 3D are more difficult for rectangular crystals, like feldspars, as for rounded crystals (e.g. Higgins, 1994; Morgan and Jerram, 2006). Alternative conversions, which assume other 3D shapes, are difficult, because the 3D shape cannot easily be inferred from 2D

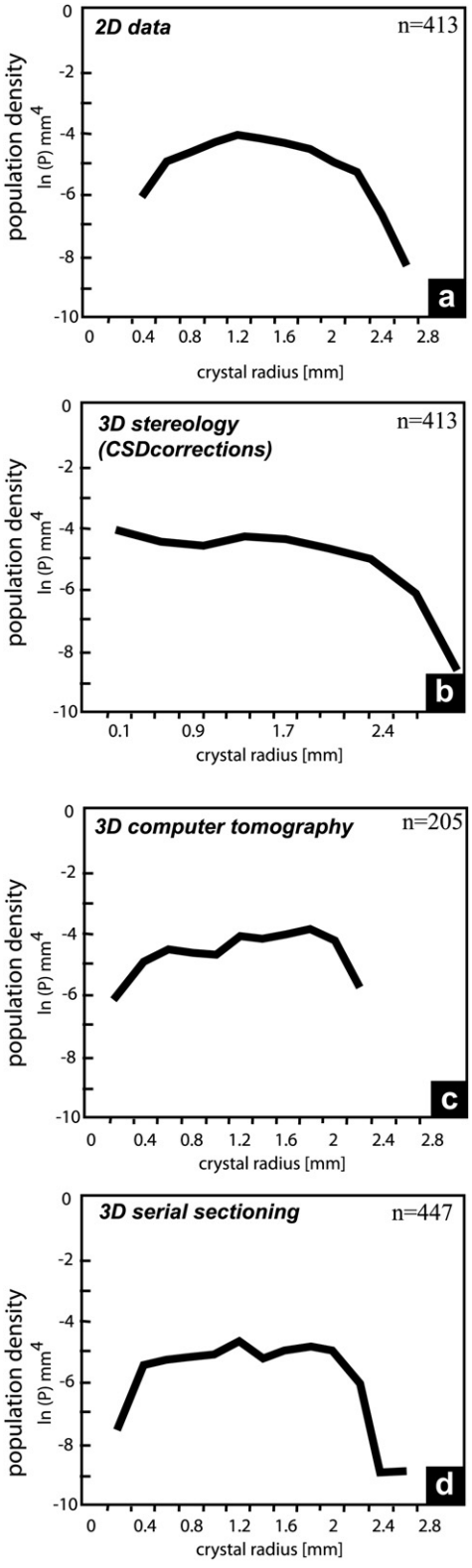

Fig. 6. Compilation of different CSDs of garnet porphyroblasts of metapelite SPi0306. (a) CSD based on 2D data as the population density. (b) Computed 3D CSD by "*CSDcorrections*", based on the data of (a). (c) Measured 3D CSD based on X-ray computed tomography. (d) Measured 3D CSD based on serial sectioning.

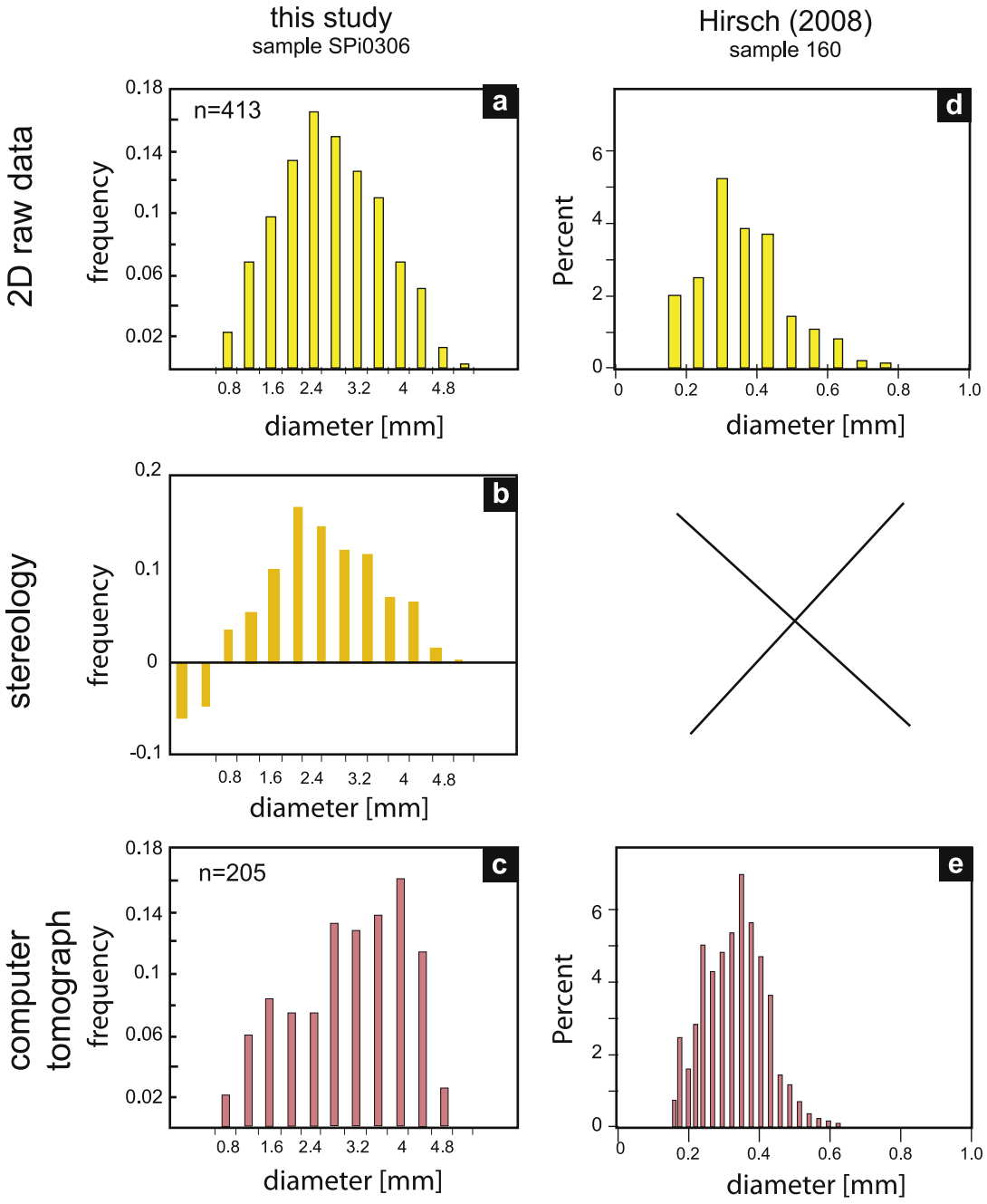

Fig. 7. Comparison of 2D and 3D CSDs from the sample SiPi0306 (see also Figs. 5 and 6) and sample 160 (Hirsch, 2008; Cashman and Ferry, 1988): (a) 2D data of sample SPi0306; (b) stereological treatment of the data of (a) using "*stripstar*"; (c) computed tomography data of sample SPi0306; (d) 2D data of sample 160, redrawn from Hirsch (2008); (e) Computed tomographic data of sample 160, redrawn after Hirsch (2008).

measurements in random oriented particles (see discussion in Higgins, 1994 and Mock and Jerram, 2005). In deformed rocks with a given shape preferred orientation, known oriented sectioning can contribute to the problem.

Table 4
Different results for garnet size measurements of sample SPi0306.

	Crystal size [mm]			Width of CSD
	Average	Maximum	Minimum	
2D (raw)	1.24	2.57	0.29	2.28
3D (computer tomography)	1.23	2.19	0.15	2.04
3D (serial sectioning)	1.21	2.42	0.04	2.39

Abbreviations: Width of the CSD = size difference between the largest and the smallest grain.

In order to describe the average grain size, the grain size distribution has to be reduced again to discrete values. In the case of unimodal distributions this step requires the description of the mean, the median and/or the mode of the population of interest. Depending on the symmetry - asymmetry of the CSD, the values between mean, median and mode can vary substantially (Fig. 1; Table 3). In general, mean and median values can be calculated in a simple way, while the calculation of the mode requires knowledge on the distribution function. In the case of symmetric Gauss shape distributions, the mean and median values are closely located to each other and also coincide with the mode (peak values) of the CSD. Therefore, all three values represent reliable grain size estimations in such distributions (Fig. 1b and c). In order to simplify the mathematical handling in the case of asymmetric CSDs, the

grain size frequency is shown as a function of class intervals with either the same width or a width related to a module α (e.g., log distribution; geometric scale, see Exner, 1972 his Table 1). Using geometric scales has the advantage that skewed distributions on the arithmetic scale can be transferred towards normal distributions, i.e., towards distributions which can mathematically be treated more easily (see as an example 3D conversion to distribution function characterisation in Kaneko et al., 2005). Log, ln and square root grain size distributions were applied in the past to facilitate the grain size parameterization (e.g. Rutter et al., 1995;

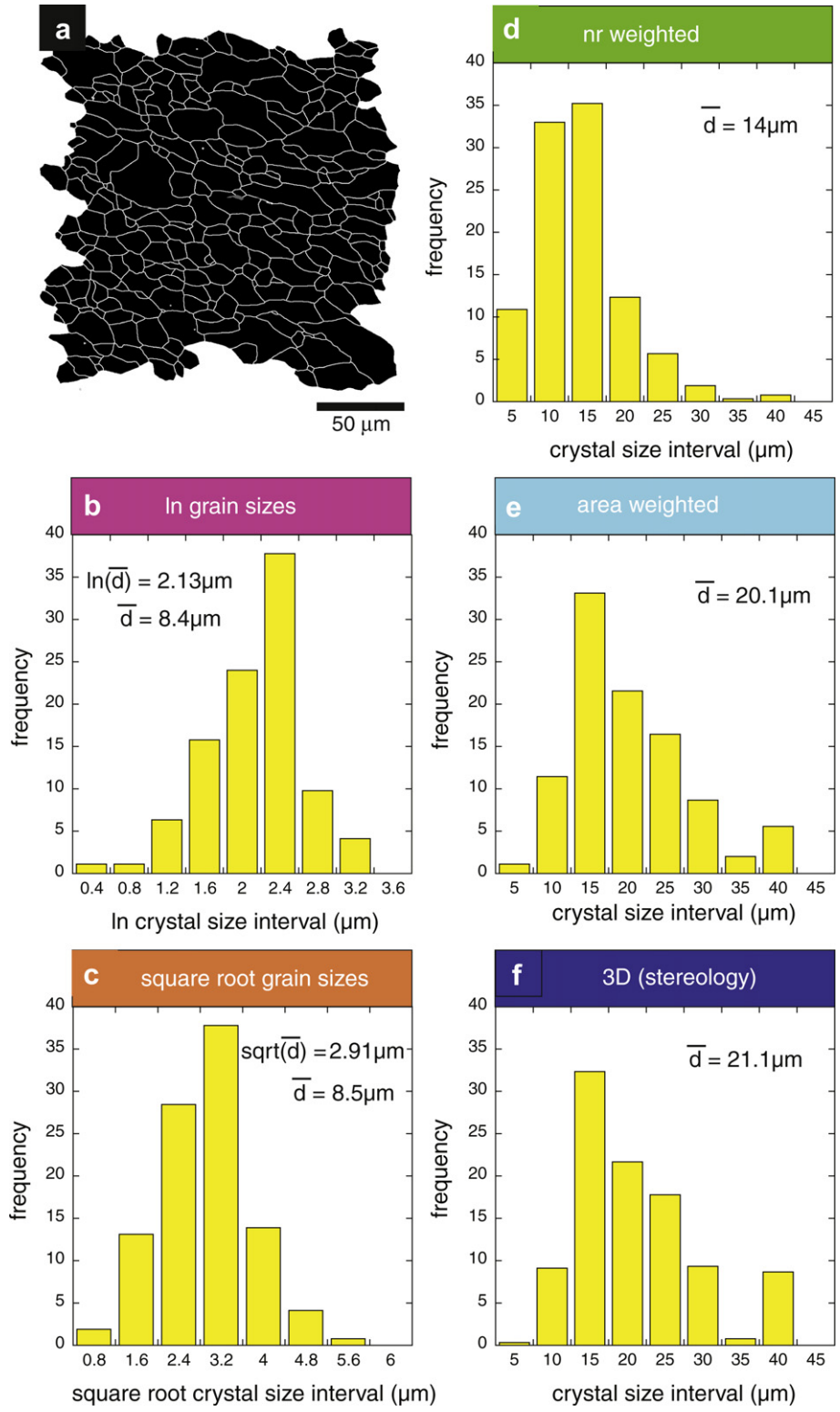

Fig. 8. Different grain size frequency diagrams using the same sample GS126 and the calculated average grain size (267 individual grains). Note the different CSDs (see Table 3 for used equations): (a) sketch of the used input (b) ln grain sizes; (c) square root grain sizes; (d) number weighted; (e) area weighted; (f) stereology (*Stripstar*).

Shimizu, 1998, de Bresser et al., 1998; Ter Heege et al., 2004, see review in Exner, 1972).

Besides these geometrical aspects, one also has to consider for which purposes the grain size data are used. In the case of rock deformation, for example, different grain size controlling processes exist, which define the dominant deformation mechanism in a rock and therefore its strength at specific deformation conditions (see Section 1.3). In order to properly correlate the rheology between experiments and nature, the statistics and distribution of the grain sizes is of great importance (De Bresser et al., 1998; Herwegh et al., 2005). For example a certain grain size class can dominate the rheology, even it is not the dominant number of grains. Therefore, the difference between volume proportion and amount of grains of a size class is relevant for data treatments of grain sizes. To incorporate the volumetric contribution of grains in a population, either 3D extrapolations are required (e.g. Heilbronner and Bruhn, 1998; Ter Heege et al., 2004; Herwegh et al., 2005) or the 2D area fraction has to be taken into consideration. With respect to the latter, Herwegh (2000; see also Ebert et al., 2007) uses the weighted grain areas to present grain size distributions (Fig. 8e; Table 3). The area frequency is calculated by counting the sum of the individual grain areas in a grain size class, while number weighted grain size distributions account for the number of grains within a class independent of the volume fraction covered by the class. Taking mean values or modes of such area weighted distributions results in larger grains compared to the number weighted ones (Table 3; Ebert et al., 2007). This is a great advantage, because the larger grains are rather close to the 3D radius of the grains (see Fig. 8; Table 3) and no assumptions on the 3D extrapolation have to be made. For the area-weighted mean, the final grain size is given as 1D length, despite being statistically counted by the grain areas (Table 3). The calculated radius or diameter is again based on Equation (1) and assumes a circular crystal shape. This simplification is reasonable for grains in recrystallized mylonites or more round-shaped minerals as for example garnet. In the case of rectangular-shaped minerals, like micas, feldspars, the reduction towards a grain diameter of a sphere or circle is an oversimplification (e.g., Higgins, 1994). Nonetheless, in comparative studies of such minerals the reduction to an equivalent circular diameter can still be helpful. Its application depends, however, on the scientific question.

Systematic variations in the average crystal size can arise by the use of different 2D methods or stereological methods (Figs. 8 and 9; Table 3). In order to evaluate potential method-dependent variations in the grain size analyses, different methods for the estimation of grain sizes were applied to a series of calcite mylonites from the Helvetic Swiss Alps (Fig. 8): (1) number counting per unit area (NCA), (2) linear intercept method (LIM), (3–4) number and area weighted equivalent circular diameters (d_{nr}, d_{area}), and (5) *StripStar* stereological analysis (d_{ss}). While number counted analysis directly delivers an average grain size, average grain sizes were calculated by taking the mean value of data derived from the intercept method and the area (d_{area}) and number weighted grain size analysis methods (Fig. 9). The different data treatments (linear intercept (LIM), number counting (d_{nr}), log-normal (d_{ln}) and square root (d_{sqrt})) require different calculations of the average in order to have comparable values (see Table 3 for the formulae). In the case of the *StripStar* grain sizes (d_{ss}; Heilbronner and Bruhn, 1998; Heilbronner, 2000) the modes of the distributions were used as the average 1D grain size. Fig. 9 shows the relationship between 1D grain sizes obtained by the linear intercept method, probably the most prominent analysis technique in monophase systems in the literature, and the grain sizes analyzed with the other techniques. The different average crystal sizes can be correlated. These correlations follow the empirical equation:

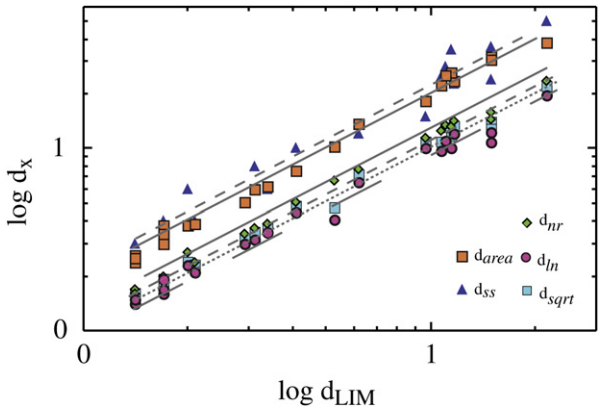

Fig. 9. Comparison of different average grain sizes using datasets from carbonate mylonites (LIM: line intecept method; d_{ss}: average crystal size using *Stripstar*; d_{area}: area weighted crystal size; d_{Nr}: number weighted average crystal size; d_{SQRT}: average crystal size of square root distribution; d_{ln}: average crystal size of logarthim distribution; see Table 3).

$$d_x = c_x \cdot d_{LIM} \tag{3}$$

where d_{LIM}, d_x and cx are the average intercept method grain size, the average grain size and a constant related to the method of interest. By using different average grain sizes from carbonate mylonites and contact metamorphic carbonates an empirical correlation matrix can be developed as shown in Table 5.

The aforementioned considerations are all based on unimodal distributions only. Nature also displays more complicated CSDs, as for example, in the form of bimodal distributions (see also Section 3.2; Fig. 5). Prominent examples for such CSD's are polyphase mixtures (e.g. Heilbronner and Bruhn, 1998) or transient deformation microfabrics (e.g. Ebert et al., 2007; Fig. 5). In such cases, different grain size distributions have to be unravelled from a bulk CSD. Estimates on the modes of the sub-CSDs can be obtained easily in area or volume-weighted frequency diagrams, as long as the individual peaks can be recognized (Fig. 5).

3.4. Applications and future prospective

As mentioned above, many different methods of grain size analysis have been chosen in the past. While they were restricted to 1D and 2D space initially, meanwhile technical progress allows exploration of the full 3D space. Hirsch (2008) compared 2D data and 3D x-ray computed tomography data of garnets. Jerram et al. (2009) correlated stereological approaches with computed tomographic data of olivine. Both studies show differences for the 2D and 3D CSD and point out the uncertainty for the interpretations. Based on such comparisons, some studies request the sole use of 3D data to extract crystal size data (e.g., Kretz, 2006). However, real 3D data acquisition and related data processing is still time and cost intensive. Also such 3D datasets as the 2D datasets have uncertainties, but the 2D ones have the advantage that they are based on cheap state of the art technology and can be combined directly with other information (e.g., element distribution maps). In order to extent the comparisons of Hirsch (2008) and Jerram et al. (2009), we compared different methods (area analysis, stereology, serial sectioning, computed tomography; Figs. 6 and 7). While some of the approaches are useful to investigate the shape of a CSD, others can only be used to estimate the average crystal size. The handling of errors is different for these datasets (see Section 3.1 and 3.2; note the given error in a CSD is more complex as any statistical parameter related to an average). More recently, the combination of CSD and average sizes is a growing research field in petrology and

Table 5
correlation factor c between mean grain sizes obtained with different analysis techniques related to Equation (3).

	NCA	*LIM*	d_{nr}	d_{area}	d_{ln}	d_{sqrt}	$d_{strip\ star}$
NCA		0.64 ± 0.03 R: 0.96	0.886 ± 0.002 R: 0.999	1.439 ± 0.009 R: 0.999	0.769 ± 0.003 R: 0.999	0.828 ± 0.003 R: 0.999	1.314 ± 0.011 R: 0.998
LIM	1.44 ± 0.06 R: 0.96		1.12 ± 0.02 R: 0.99	2.09 ± 0.09 R: 0.96	0.90 ± 0.02 R: 0.98	1.01 ± 0.02 R: 0.99	2.21 ± 0.09 R: 0.96
d_{nr}	1.129 ± 0.003 R: 0.999	0.72 ± 0.03 R: 0.95		1.624 ± 0.014 R: 0.998	0.869 ± 0.002 R: 0.999	0.935 ± 0.002 0.999	1.482 ± 0.015 R: 0.997
d_{area}	0.693 ± 0.005 R: 0.999	0.45 ± 0.02 R: 0.96	0.614 ± 0.005 R: 0.998		0.533 ± 0.006 R: 0.998	0.574 ± 0.006 R: 0.998	0.912 ± 0.009 R: 0.998
d_{ln}	1.297 ± 0.006 R: 0.999	0.83 ± 0.04 R: 0.95	1.150 ± 0.003 R: 0.999	1.866 ± 0.020 R: 0.997		1.076 ± 0.001 R: 0.999	1.703 ± 0.20 R: 0.997
d_{sqrt}	1.207 ± 0.004 R: 0.999	0.77 ± 0.04 R: 0.95	1.070 ± 0.002 R: 0.999	1.735 ± 0.017 R: 0.998	0.930 ± 0.001 R: 0.999		1.584 ± 0.017 R: 0.997
$d_{strip\ star}$	0.759 ± 0.007 R: 0.998	0.49 ± 0.02 R: 0.96	0.672 ± 0.007 R: 0.997	1.093 ± 0.010 R. 0.998	0.584 ± 0.007 R. 0.997	0.628 ± 0.007 R: 0.997	

Error: error of the best fit as seen in Fig. 9; R: correlation coefficient.

structural geology (e.g., Berger et al., 2010). Particularly, the combination of CSD and mean grain size allows to distinguish between nucleation and growth processes and coupled grain coarsening (e.g., Berger et al., 2010; Brodhag et al., 2011; Herwegh et al., in this volume). The resulting datasets must not only be internally comparable within a study comprising considerable grain size variations, but should also be comparable to older studies performed on natural or experimental samples.

One of the most fundamental tasks in the field of grain size analysis is the identification of a potential bimodal CSD, which requires robust information on the shape of CSD. In studies that concentrate on the average grain size (e.g., paleopiezometry), it is mandatory to make sure that no bimodal grain size distribution exists. Particularly in the case of a small number of large grains with volumetrically significant contributions to the aggregate's volume, the bimodal character of the CSD might be hidden by solely generating number weighted grain size datasets (see above and Heilbronner and Bruhn, 1998). Therefore, area-weighted or volumetric grain size data should generally be used. In the case of a bimodal character of the distribution, the modes of the different peaks have to be used to extract useful average data. Alternatively, one could also apply deconvolution software to extract the compartments of the different grain size classes contributing to a specific grain population. The latter step is necessary for all applications in which the contribution of each grain size interval is of relevance in order to estimate the bulk property of the entire aggregate. Potential applications with this respect are composite flow laws, where for each grain size interval the contributions of the deformation mechanisms involved have to be calculated (e.g. Ter Heege et al., 2004; Herwegh et al., 2005). Depending on the applied grain size analysis techniques, variations in grain size up to a factor of 2 are possible (Table 5). Without correcting for the used grain size analysis method, these variations will propagate and therefore would increase the error. It is therefore always crucial to carefully check how grain sizes are estimated and how the own data can be adapted to previous approaches.

4. Conclusion and outlook

Grain size analyses are used in several fields of geosciences. Grain sizes in monomineralic deformed systems have been often estimated with 1D methods (i.e. line intercept methods). However, the quantification of deformed and undeformed, polyphase systems is more efficient with image analysis techniques (2D). In addition, comparison between 2D and 3D methods in polymineralic systems are now available to test the quality of such data (e.g., Hirsch, 2008; Jerram et al., 2009, this study). These results are an important improvement for grain size analysis in all material. In studies of metamorphic microstructures, combining average values with CSD will be more used in the future, because the matrix is as important as the one of the porphyroblasts, since the grain boundary network of the matrix provides the transport pathways for the nutrients required for the growth of the porphyroblasts (e.g., Carlson and Gordon, 2004; Brodhag et al., 2011). In the future, grain size of prophyroblasts may be more often measured with 3D methods, as computed tomography gets accessible, whereas matrix grain size will measured by 2D image analysis. Comparing different methods, we propose, area weighted grain size are the most useful 2D method for average grain sizes.

References

Austin, N.J., Evans, B., 2007. Paleowattmeters: a scaling relation for dynamically recrystallized grain size. Geology 35, 343–346.
Austin, N.J., Evans, B., 2009. The kinetics of microstructural evolution during deformation of calcite. Journal of Geophysical Research-Solid Earth 114, B09402.

Barraud, J., 2006. The use of watershed segmentation and GIS software for textural analysis of thin sections. Journal of Volcanology and Geothermal Research 154, 17–33.
Berger, A., Herwegh, M., 2004. Grain coarsening of contact metamorphic carbonates: effects of second phase particles, fluid flow and thermal perturbations. Journal of Metamorphic Geology 22, 459–474.
Berger, A., Roselle, G., 2001. Crystallization processes in migmatites. American Mineralogist 86, 215–224.
Berger, A., Brodhag, S.H., Herwegh, M., 2010. Reaction-induced nucleation and growth v. grain coarsening in contact metamorphic, impure carbonates. Journal of Metamorphic Geology 28, 809–824.
Bjørk, T.E., Mair, K., Austrheim, H., 2009. Quantifying granular material and deformation: advantages of combining grain size, shape, and mineral phase recognition analysis. Journal of Structural Geology 31, 637–653.
Boorman, S., Boudreau, A., Kruger, F., 2004. The lower zone-critical zone transition of the Bushveld complex: a quantitative textural study. Journal of Petrology 45, 1209–1235.
Brodhag, S.H., Herwegh, M., Berger, A., 2011. Static grain growth in polymineralic carbonates. Journal of Structural Geology 33, 698–712.
Bryon, D.N., Atherton, M.P., Hunter, R.H., 1995. The interpretation of granitic textures from serial thin sectioning, image-analysis and 3 dimensional reconstruction. Mineralogical Magazine 59, 203–211.
Carlson, W.D., 1989. The significance of intergranular diffusion to the mechanisms and kinetics of porphyroblast crystallization. Contribution to Mineralogy and Petrology 103, 1–24.
Carlson, W.D., 2010. Porphyroblast crystallization: linking processes, kinetics, and microstructures. International Geology Review, 1–40.
Carlson, W.D., Gordon, C.L., 2004. Effects of matrix grain size on the kinetics of intergranular diffusion. Journal of Metamorphic Geology 22, 733–742.
Cashman, K.V., Ferry, J.M., 1988. Crystal Size distrubution (CSD) in rocks and kinetics and dynamics of crystallization. III. Metamorphic crystallization. Contribution to Mineralogy and Petrology 99, 401–415.
Cashman, K.V., Marsh, B.D., 1988. Crystal size distribution (CSD) in rocks and the kinetics and dynamics of crystallisation II. Makaopuhi lava lake. Contribution to Mineralogy and Petrology 99, 292–305.
Cooper, M.R., Hunter, R.H., 1995. Precision serial lapping, imaging and three-dimensional reconstruction of minus-cement and post-cementation intergranular pore-systems in the Penrith Sandstone of north-western England. Mineralogical Magazine 59, 213–220.
De Bresser, J.H.P., Peach, C., Reijs, J., Spiers, C., 1998. On dynamic recrystallization during solid state flow: effects of stress and temperature. Geophysical Research Letters 25, 3457–3460.
De Bresser, J.H.P., Ter Heege, J.H., Spiers, C.J., 2001. Grainsize reduction by dynamic recrystallization: can it result in major rheological weakening? International Journal of Earth Sciences 90, 28–45.
De Hoff, R.T., 1991. A geometrically general theory of diffusion controlled coarsening. Acta Metallica Materialia 39, 2349–2360.
Denison, C., Carlson, W.D., 1997. Three-dimensional quantitative textural analysis of metamorphic rocks using high-resolution computed X-ray tomography: Part II. Application to natural samples. Journal of Metamorphic Geology 15, 45–57.
Denison, C., Carlson, W.D., Ketcham, R.A., 1997. Three dimensional quantitative textural analysis of metamorphic rocks using high resolution computed X-ray tomography: part I. Methods and techniques. Journal of Metamorphic Geology 15, 45–57.
Eberl, D.D., Drits, V.A., Srodon, J., 1998. Deducing growth mechanisms for minerals from the shapes of crystal size distributions. American Journal of Science 298, 499–533.
Eberl, D.D., Kile, D.E., Drits, V.A., 2002. On geological interpretations of crystal size distributions: constant vs. Proportionate growth. American Mineralogist 87, 1235–1241.
Ebert, A., Herwegh, M., Pfiffner, O.A., 2007. Cooling induced strain localization in carbonate mylonites within a large-scale shear zone (Glarus thrust, Switzerland). Journal of Structural Geology 29, 1164–1184.
Ebert, A., Herwegh, M., Berger, A., Pfiffner, O.A., 2008. Grain coarsening maps for polymineralic carbonate mylonites: a calibration based on data from different Helvetic nappes (Switzerland). Tectonophysics 457, 128–142.
Ebert, A., Gnos, E., Ramseyer, K., Spandler, C., Fleitmann, D., Bitzios, D., Decrouez, D., 2010. Provenance of marbles from Naxos based on microstructural and geochemical characterization. Archaeometry 52, 209–228.
Evans, B., Renner, J., Hirth, G., 2001. A few remarks on the kinetics of static grain growth in rocks. International Journal of Earth Sciences (Geologische Rundschau) 90, 88–103.
Exner, H.E., 1972. Analysis of grain- and particle-size distributions in metallic materials. International Metallica Reviews 17, 25–42.
Galwey, A.K., Jones, K.A., 1963. An attempt to determine the mechanism of a natural mineral-forming reaction from examination of the products. Journal of the Chemical Society (London), 5681–5686.
Gleason, G.C., Tullis, J., 1993. Improving flow laws and piezometers for quartz and feldspar aggregates. Geophysical Research Letters 20, 2111–2114.
Gleason, G.C., Tullis, J., Heidelbach, F., 1993. The role of dynamic recrystallization in the development of lattice preferred orientations in experimentally deformed quartz aggregates. Journal of Structural Geology 15, 1145–1168.
Gualda, G.A.R., 2006. Crystal size distributions derived from 3D datasets: sample size versus uncertainties. Journal of Petrology 47, 1245–1254.
Heilbronner, R., 2000. Automatic grain boundary detection and grain size analysis using polarization micrographs or orientation images. Journal of Structural Geology 22, 969–982.
Heilbronner, R., Bruhn, D., 1998. The influence of three dimensional grain size distributions on the rheology of polyphase rocks. Journal of Structural Geology 20, 695–705.
Herwegh, M., 2000. A new technique to automatically quantify microstructures of fine grained carbonate mylonites: two step etching combined with SEM imaging and image analysis. Journal of Structural Geology 22, 391–400.
Herwegh, M., Berger, A., 2003. Differences in grain growth of calcite: a field-based modeling approach. Contribution to Mineralogy and Petrology 145, 600–611.
Herwegh, M., Berger, A., 2004. Deformation mechanisms in second-phase affected microstructures and their energy balance. Journal of Structural Geology 26, 1483–1498.
Herwegh, M., Handy, M.R., 1996. The evolution of high temperature mylonitic microfabrics: evidence from simple shearing of a quartz analogue (norcamphor). Journal of Structural Geology 18, 689–710.
Herwegh, M., Pfiffner, O.A., 2005. Tectono-metamorphic evolution of a nappe stack: a case study of the Swiss Alps. Tectonophysics 404, 55–76.
Herwegh, M., De Bresser, J.H.P., Ter Heege, J.H., 2005. Combining natural microstructures with composite flow laws: an improved approach for the extrapolation of lab data to nature. Journal of Structural Geology 27, 503–521.
Herwegh, M., Berger, A., Ebert, A., Brodhag, S., 2008. Discrimination of annealed and dynamic fabrics: consequences for strain localization and deformation episodes of large-scale shear zones. Earth and Planetary Science Letters 276, 52–61.
Herwegh, M., Linckens, J., Ebert, A., Berger, A., Brodhag, S. The role of second phases for controlling microstructural evolution in polymineralic rocks. Journal of Structural Geology, in this volume.
Higgins, M.D., 1994. Numerical modeling of crystal shapes in thin-sections: estimation of crystal habit and true sizes. American Mineralogist 79, 113–119.
Higgins, M.D., 2000. Measurement of crystal size distribution. American Mineralogist 85, 1105–1116.
Higgins, M.D., 2006. Quantitative Textural Measurements in Igneous and Metamorphic Petrology. Cambridge University Press, Cambridge.
Higgins, M.D., Roberge, J., 2007. Three magmatic components in the 1973 eruption of Eldfell volcano, Iceland: evidence from plagioclase crystal size distribution (CSD) and geochemistry. Journal of Volcanic and Geothermal Research 161, 257–260.
Hirsch, D.M., 2008. Controls on porphyroblast size along a regional metamorphic field gradient. Contribution to Mineralogy and Petrology 155, 401–415.
Hirth, G., Tullis, J., 1992. Dislocation creep regimes in quartz aggregates. Journal of Structural Geology 14, 145–160.
Hobbs, B.E., 1968. Recrystallization of single crystals of quartz. Tectonophysics 6, 353–401.
Jerram, D.A., Higgins, M., 2007. 3D analysis of rock textures: quantifying igneous microstructures. Elements 3, 239–245.
Jerram, D.A., Kent, A.J.R., 2006. An overview of modern trends in petrography: textural and microanlysis of igneous rocks. Journal of Volcanology and Geothermal Research 154, VII–IX.
Jerram, D.A., Mock, A., Davis, G.R., Field, M., Brown, R.J., 2009. 3D crystal size distributions: a case study on quantifying olivine populations in kimberlites. Lithos 112S, 223–235.
Jones, K.A., Galwey, A.K., 1966. Size distribution, composition, and growth kinetics of garnet crystals in somemetamorphic rocks from the west of Ireland. Quaterly Journal of the Geological Society of London 122, 29–44.
Kaneko, Y., Tsunogae, T., Miyano, T., 2005. Crystal-size distributions of garnets in metapelites from the northeastern Bushveld contact aureole, South Africa. American Mineralogist 90, 1422–1433.
Ketcham, R.A., 2005. Computational methods for quantitative analysis of three-dimensional features in geological specimens. Geosphere 1, 32–41.
Kile, D.E., Eberl, D.D., Hoch, A.R., Reddy, M.M., 2000. An assessment of calcite crystal growth mechanisms based on crystal size distributions. Geochimica et Cosmochimica Acta 64, 2937–2950.
Kohlstedt, D.L., Evans, B., Mackwell, S.J., 1995. Strength of the lithosphere: constraints imposed by laboratory experiments. Journal of Geophysical Research-Solid Earth 100, 17587–17602.
Kretz, R., 2006. Shape, size, spatial distribution and composition of garnet crystals in highly deformed gneiss of the Otter Lake area, Québec, and a model for garnet crystallization. Journal of Metamorphic Geology 24, 431–449.
Marsh, B.D., 1988. Crystal Size distribution (CSD) in rocks and kinetics and dynamics of crystallization. 1. Theory. Contribution to Mineralogy and Petrology 99, 277–291.
Marsh, B.D., 1998. On the interpretation of crystal size distributions in magmatic systems. Journal of Petrology 39, 553–599.
Means, W.D., 1981. The concept of steady-state foliation. Tectonophysics 78, 179–199.
Miyake, A., 1998. Monte Carlo simulation of normal grain growth in 2- and 3-dimensions: the lattice-model independent grain size distribution. Contribution to Mineralogy and Petrology 130, 121–133.
Miyazaki, K., 1991. Ostwald ripening of garnet in high P/T metamorphic rocks. Contribution to Mineralogy and Petrology 108, 118–128.
Mock, A., Jerram, D.A., 2005. Crystal size distributions (CSD) in three dimensions: insights from the 3D reconstruction of a highly porphyritic rhyolite. Journal of Petrology 46, 1525–1541.
Morgan, D.J., Jerram, D.A., 2006. On estimating crystal shape for crystal size distribution analysis. Journal of Volcanic and Geothermal Research 154, 1–7.
Platt, J.P., Behr, W.M., 2011. Grain size evolution in ductile shear zones: implications for strain localization and the strength of the lithosphere. Journal of Structural Geology 33, 537–550.
Poirier, J.P., 1985. Creep of Crystals. Cambridge University Press, Cambridge, UK.

Post, A., Tullis, J., 1999. A recrystallized grain size piezometer for experimentally deformed feldspar aggregates. Tectonophysics 303, 159–173.
Randolph, A.D., Larson, M.A., 1971. Theory of Particulate Processes. Academic Press, New York, 251 pp.
Rutter, E.H., 1995. Experimental study of the influence of stress, temperature, and strain on the dynamic recrystallization of Carrara marble. Journal of Geophysical Research-Solid Earth 100, 24651–24663.
Schmid, S.M., 1975. The Glarus overthrust: field evidence and mechanical model. Eclogae Geologica Helvetica 68, 251–284.
Schmid, S.M., Paterson, M.S., Boland, J.N., 1980. High temperature flow and dynamic recrystallization in Carrara marble. Tectonophysics 65, 245–280.
Schwarz, J.O., 2008. Porphyroblasts: Textural Analysis and a Genetic Model for Garnet-Bearing Metasediments, PhD thesis, Univ. Bern. 156 pp.
Schwarz, J.O., Engi, M., Berger, A., 2011. Porphyroblast crystallization kinetics: the role of the nutrient production rate. Journal of Metamorphic Geology 29, 497–512.
Shimizu, I., 1998. Stress and temperature dependence of recrystallized grainsize: a subgrain misorientation model. Geophysical Research Letters 25, 4237–4240.
Srinivansan, S., Russ, J.C., Scattergood, R.O., 1991. Grain size measurements using the point-sampled intercept technique. Scripta Metallica et Materialia 25, 931–934.
Stipp, M., Tullis, J., 2003. The recrystallized grain size piezometer for quartz. Geophysical Research Letters 30, 2088.
Stipp, M., Tullis, J., Scherwath, M., Behrmann, J.H., 2010. A new perspective on paleopiezometry: dynamically recrystallized grain size distributions indicate mechanism changes. Geology 38, 759–762.
Storti, F., Billi, A., Salvini, F., 2003. Particle size distribution in natural carbonate fault rocks: insights for non-self-similar cataclasis. Earth and Planetary Science Letters 206, 173–186.
Ter Heege, J.H., De Bresser, J.H.P., Spiers, C.J., 2004. Composite flow laws for crystalline materials with log-normally distributed grain size: theory and application to olivine. Journal of Structural Geology 26, 1693–1705.
Twiss, R.J., 1977. Theory and applicability of a recrystallized grain size palaepiezometer. Pure and Applied Geophysics 115, 227–244.
Underwood, E.E., 1968. Particle size distributions. In: DeHoff, R.T., Rhines, F.N. (Eds.), Quantitative Microscopy. MacGraw-Hill, New York, p. 149.
Vernon, R.H., 2004. A Practical Guide to Rock Microstructure. University Press Cambridge, Cambridge.
Walker, A.N.E.H., Rutter, E.H., Brodie, K.H., 1990. Experimental Study of Grain-size Sensitive Flow of Synthetic, Hot-pressed Calcite Rocks. In: Geological Society of London, Special Publications, vol. 54 259–284.